UDK 691.714:004.414.23
Original scientific article/Izvirni znanstveni članek

ISSN 1580-2949
Mater. Tehnol.

ABSORBED ENERGY MODELING OF HYPOEUTECTOID STEELS USING LINEAR REGRESSION AND GENETIC PROGRAMMING TAKING INTO ACCOUNT CONTINUOUS CASTING PARAMETERS

MODELIRANJE ABSORBIRANE ENERGIJE HIPOEVTEKTOIDNIH JEKEL Z UPORABO LINEARNE REGRESIJE IN GENETSKEGA PROGRAMIRANJA Z UPOŠTEVANJEM PARAMETROV KONTINUIRNEGA LITJA

Miha Kovačič[1,2,3], Uroš Župerl[4], Gašper Gantar[3,5]

[1]Štore Steel, Železarska cesta 3, 3220 Štore, Slovenia
[2]University of Ljubljana, Faculty of Mechanical Engineering, Aškerčeva cesta 6, 1000 Ljubljana, Slovenia
[3]College of Industrial Engineering, Mariborska cesta 2, 3000 Celje, Slovenia
[4]University of Maribor, Faculty of Mechanical Engineering, Smetanova 17, 2000 Maribor, Slovenia
[5]Faculty of Environmental Protection, Trg mladosti 7, 3320 Velenje, Slovenia

Prejem rokopisa – received: 2024-12-18; sprejem za objavo – accepted for publication: 2025-09-18

doi:10.17222/mit.2024.1356

Štore Steel Ltd. is one of the major flat spring steel producers in Europe, producing several hundred steel grades with different chemical compositions. (180 × 180) mm billets are cast using a continuous casting machine with a 9-m radius. The macrostructure of the billets influence the mechanical properties of rolled material. For impact testing, standard test pieces are obtained from the rolled material at a defined location and orientation. Accordingly, the reduction ratio is also essential. Based on 2243 V-notch test pieces obtained from rolled materials produced in several batches between January 2019 and May 2024, models for predicting the absorbed energy of the rolled material at temperatures ranging from –60 °C to 20 °C were developed using linear regression and genetic programming. The models incorporated parameters such as chemical composition (contents of C, Si, Mn, S, Cr, Mo, Ni, Al, and V), casting conditions (average casting temperature, mold water flow, average difference between input and output mold cooling water temperature, average cooling water flow and pressure in three zones of secondary cooling), as well as the width and thickness of the rolled bars and test temperature. The genetic programming model outperformed the linear regression model.

Keywords: absorbed energy, Charpy impact test, V-notch test pieces, casting parameters, modeling, linear regression, genetic programming

Štore Steel d.o.o. je eden večjih proizvajalcev ploščatih vzmetnih jekel v Evropi, kjer proizvajajo več sto kvalitet jekel z različnimi kemičnimi sestavami. Gredice (180 mm x 180) mm so ulite s kontinuirno livno napravo s polmerom 9 m. Makrostruktura gredic vpliva na mehanske lastnosti valjanega materiala. Za udarne preskuse se preizkušanci pridobijo iz valjanega materiala z določene lokacije in usmerjenosti. Skladno s tem je bistvena tudi redukcija. Na podlagi 2243 preizkušancev z V-zarezo, pridobljenih iz valjanega materiala iz šarž, proizvedenih od januarja 2019 do maja 2024, kemične sestave (vsebnost C, Si, Mn, S, Cr, Mo, Ni, Al in V), parametrov litja (povprečna temperatura litja, pretok vode v kokili, povprečna razlika med vhodno in izhodno temperaturo hladilne vode v kokili, povprečni pretok hladilne vode in tlaka v treh conah sekundarnega hlajenja), širine in debeline valjane palice ter preskusna temperatura so bili razviti modeli linearne regresije in genetskega programiranja za napoved absorbirane energije valjanega materiala od –60 °C do 20 °C. Model genetskega programiranja je natančnejši od modela linearne regresije.

Ključne besede: absorbirana energija, Charpy test, preizkušanci z V-zarezo, livni parametri, modeliranje, linearna regresija, genetsko programiranje

1 INTRODUCTION

The Charpy impact test is a standard procedure for determining the energy absorbed by a material during instantaneous fracture[1]. It is calculated using the potential energy lost by the pendulum during the fracture of a specially designed test piece with a notch. The notch effect provides the reproducibility of the results. It can be V or U shaped. The test can be performed at different temperatures of the test piece. Consequently, several parameters influence the absorbed energy during a Charpy impact test:

- material: its chemical composition,[2–7] segregations,[5,6] precipitation,[8] non-metallic inclusions,[9] microstructure,[4,10–15] macrostructure,[4,16] heat treatment;[3,10,13,15]
- geometry: geometry of the test piece, notch;[17–20]
- equipment: lubrication,[21] calibration;[1,3,21]
- environment: ambient temperature, humidity, draft;[22,5,10,11] and

*Corresponding author's e-mail:
miha.kovacic@store-steel.si (Miha Kovačič)

- procedure: location,[17,23] orientation of the test pieces relative to the sample,[17,23] test piece positioning, machining, test temperature.[5,8,10,11,13,16,22,24–26]

It is clear that with all possible absorbed energy variations, its prediction is a challenging task. As a result, when attempting to predict absorbed energy, researchers analyze their effects. Researches are sometimes limited to only individual steel grades,[5,8,10–13,16,17,24–26] but at the same time we can find a small number of industrial studies.[22] They are often related to the welding process[4,12,26,27] and the associated hydrogen charging.[25] Finite element methods (FEM)[4,11,18,20] and artificial intelligence methods such as neural networks,[3,28–30] fuzzy logic,[3,30] and evolutionary methods (e.g., genetic algorithm)[29] are also used for the prediction of absorbed energy.

This article presents the prediction of absorbed energy, based on 2243 V-notch test pieces obtained from rolled material produced in several batches of hypoeutectoid steels at Štore Steel Ltd. between January 2019 and May 2024, using linear regression and genetic programming. It has to be emphasized that for the first time casting parameters (average casting temperature, mold water flow, average difference between input and output mold cooling water temperature, average cooling water flow and pressure in three zones of secondary cooling) and the corresponding macrostructure of the cast semi-product are taken into account for the prediction of absorbed energy. The goal is to understand the influence of casting parameters and the macrostructure of the cast billets on the absorbed energy determined using the Charpy impact test (ISO 148-1).

The data collection is presented at the beginning of the article. In the following sections, an attempt to predict the absorbed energy using linear regression and genetic programming is presented. The results are also presented. The conclusion also provides guidelines for the future.

2 MATERIALS AND METHODS

The reduction at the Štore Steel plant begins with scrap melting in an electric arc furnace, followed by tapping, ladle treatment (i.e., secondary metallurgy), and continuous casting of billets measuring (180 × 180) mm, using a 9-m radius continuous casting machine. Solidification of the melt takes place during primary (cooling in water cooled copper mold), secondary (cooling with water sprays) and tertiary (radiation in air) cooling.

Secondary cooling consists of 3 zones. The spray ring in zone 1 is connected directly below the mold support. It consists of 3 rows with spray nozzles which allow uniform cooling of a billet when it leaves the mold. The upper row is equipped with 8 nozzles, the lower two rows with 4 nozzles. The spray ring system in zone 2 is mounted on the structure in the cooling chamber. It consists of 2 parts – zone 2a and zone 2b. Zones 2a and 2b consist of 8 and 6 rows with spray nozzles, respectively. 5 rows are installed in zone 3. All rows are equipped with 4 nozzles.

The continuous casting machine and its cooling zones are schematically presented in **Figure 1**.

The typical macrostructure of a billet consists of:

- the chill zone (a rapidly cooled area with a fine structure at the surface of the billet),
- the columnar, dendritic zone (a tree-like pattern with branches, which becomes more pronounced at high superheat during casting) and
- the equiaxed zone (the zone in the core of the billet where the grains are of approximately the same size in all directions).

The billets can undergo additional heat treatment or be cooled under hoods to reduce residual stresses that might cause internal defects. After exiting the reheating furnace, the billets go through a descaling device and a

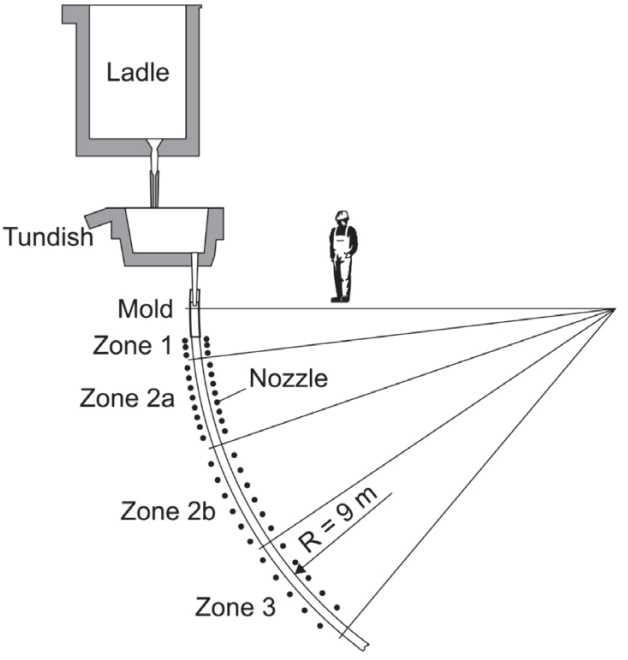

Figure 1: Continuous casting machine and its cooling zones

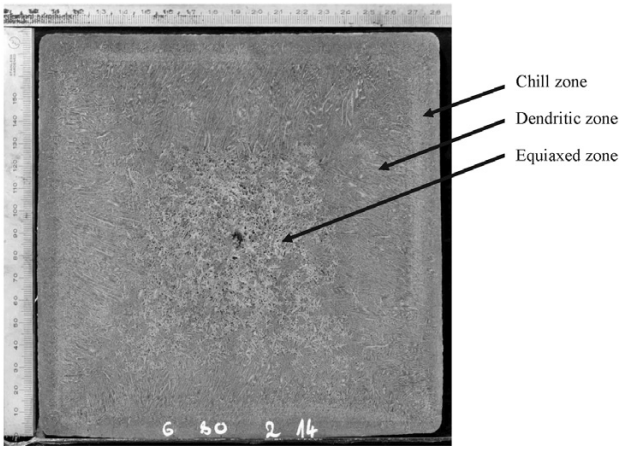

Figure 2: Typical macrostructure of a continuously cast billet

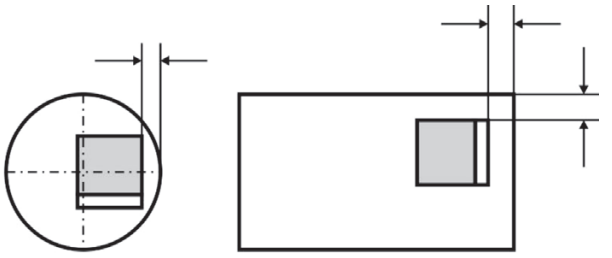

Figure 3: Location of test pieces for impact testing for round and rectangular bars (according to ISO 377)

duo reversible rolling stand with 800-mm diameter rolls. The rolled material undergoes 7 passes. The final rolling diameters achieved using the same rolling stand range from 95 mm to 110 mm.

Before the material enters the continuous rolling line with 460-mm diameter rolls (700-mm length), it is rolled using a duo reversible rolling stand with 650-mm diameter rolls. After exiting the duo reversible stand, where the material is subjected to 5 passes (the last is a by-pass), the material cools down as the rolling temperature is achieved. The temperature is measured using an infrared pyrometer.

The continuous rolling line itself consists of a descaling device, 6 horizontal and 4 vertical stands, three hot shears – of which two are used for cutting the first and the last end of the rolled bar, while the third is used for cutting the final dimensions before the material enters the cooling bed. The rolled bars can then be straightened, examined for inner soundness and surface quality, cut, sawn, chamfered, drilled, and peeled.

Samples were obtained from rolled bars (without additional heat treatment) with diameters from 18 mm to 110 mm and rectangular bars with thickness values from 8 mm to 73 mm and width values from 45 mm to 200 mm from the middle billet of the rolling lot. Preparation of the samples and test pieces was conducted according to ISO 377 (Steel and steel products – Location and preparation of samples and test pieces for mechanical testing) and ISO 148-1 (Metallic materials – Charpy, pendulum impact test – Part 1: Test method). The location of the test pieces for impact testing for round and rectangular bars (according to ISO 377) is shown in **Figure 3**. The offset of the sample from the bar surface depends on the dimensions of the bars (i.e., diameter, width and thickness). The notch is always oriented away from the center of the bar.

Based on the required locations for impact testing (ISO 377), the locations of the test pieces and the equiaxed zone (grey) of the billets at different rolled bar diameters are presented in **Figure 4**. It is clear that the notch at larger diameters is partly located already in the dendritic zone of the billet (above ϕ40 mm). On the other hand, at lower diameters, the notch is closer to the center of the bar and is influenced by the centerline and central porosity.

The Charpy pendulum impact test was performed by the same operator, using the same toughness testing machine (FIT 30-1, AVK – Anyaguizsgalo Keszulekek Gyara Budapest, a range of 0–245 J) in accordance with ISO 148-1.

Based on 2243 V-notch test pieces obtained from the rolled material (without additional heat treatment) from batches produced between January 2019 and May 2024, the following data were collected:

- Chemical composition: contents of carbon (C), silicon (Si), manganese (Mn), sulfur (S), chromium (Cr), molybdenum (Mo), nickel (Ni), aluminium (Al) and vanadium (V).
- Casting parameters:
  - Average casting temperature [°C] (CTEMP).
  - Average cooling water flow in the mold [L/min] (QMOLD).
  - Average difference between input and output mold cooling water temperatures [°C] (DELTAT).
  - Average cooling water flow [L/min] and pressure [bar] in the first (directly below the mold) (QZ1, PZ1), second (QZ2, PZ2) and third zone (QZ3, PZ3) of secondary cooling.
- Rolled material geometry:
  - Width [mm] (WIDTH).
  - Thickness [mm] (THICK).
- Test temperature (TEMP).

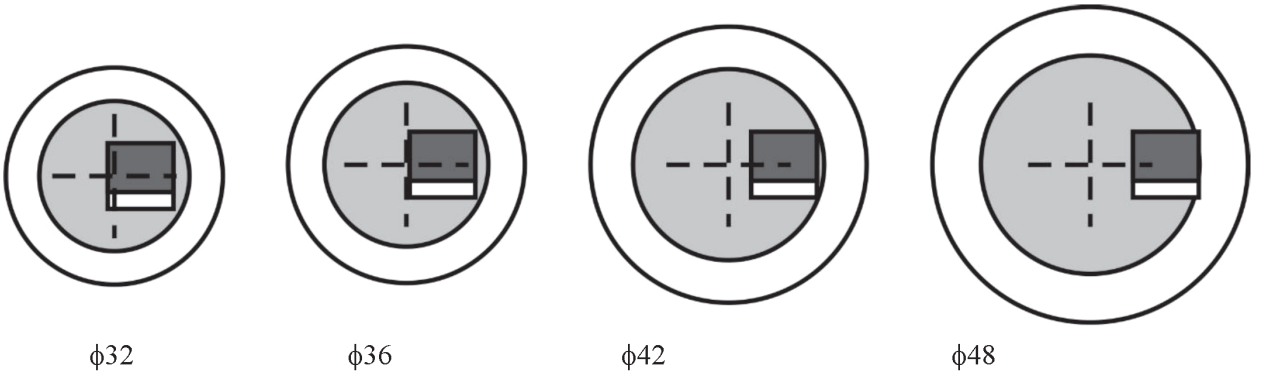

Figure 4: Locations of test pieces and equiaxed zone (grey) of the billets at different rolled bar diameters in the case of typical secondary cooling parameters

- Rolled material (without additional heat treatment) absorbed energy from –60 to 20 °C for V-notch test pieces [J] (KV).

The numbers of V-notch test pieces for individual steel grades are presented in **Table 1**.

Table 1: Number of V-notch test pieces for individual steels

Steel grade	Number of V-notch test pieces
16MnCr5	1
16MnCrS5	16
18CrNiMo7-6	2
20MnV6	934
20NiCrMo2	6
23MnNiCrMo5-2	36
25CrMo4	4
28MnCrB7	78
28MnCrNiB	13
30MnB5	19
38MnVS6	143
41Cr4	1
41CrS4	2
42CrMo4	14
42CrMoS4	56
46MnVS5	13
C22	5
C45	25
C45S	15
P460NH	197
S235J2	22
S235JR	8
S355J2	572
C35S	25
25CrMoS4	30
33MnCrNiMoB5	4
33MnCrB5-2	2
SUM	2243

In all cases, rolling was completed on the continuous rolling line, with an entry temperature consistently set at 910 °C. Cooling of all pieces was carried out in the same manner, on a cooling bed. It is assumed that, for given dimensions, the cooling conditions on the cooling bed were identical. Consequently, the influence of the microstructure of the same material and dimension, under the same rolling and cooling conditions, can be considered negligible.

3 MODELING OF ABSORBED ENERGY

On the basis of the collected data, the prediction of the absorbed energy for V-notch test pieces was conducted using linear regression and genetic programming. For the fitness function, the average relative deviation between the predicted and experimental data was selected.

3.1 Modeling of absorbed energy using linear regression

On the basis of the linear regression results, it is possible to conclude that the model significantly predicts the absorbed energy ($p < 0.05$, ANOVA) and that 41.2 % of total variances can be explained with independent variable variances (R-square). Most parameters are statistically significantly influential except for carbon (C), aluminium (Al) and vanadium (V) contents and the thickness (THICK) of the rolled bars ($p > 0.05$).

The linear regression model is as follows:

$$\begin{aligned}KV = &-274.29\cdot C - 15.60\cdot Si - 13.54\cdot Mn - \\ &333.62\cdot S - -7.56\cdot Cr + 157.02\cdot Mo - 97.12\cdot Ni \\ &+ 261.56\cdot Al - 35.63\cdot V - 0.095\cdot CTEMP - \\ &-0.573\cdot QMOLD - 2.00\cdot DELTAT - 8.48\cdot QZ1 - \\ &6.81\cdot PZ1 + 4.12\cdot QZ2 + 3.40\cdot PZ2 + \\ &2.55\cdot QZ3+11.10\cdot PZ3 + 0.14\cdot WIDTH - \\ &0.08\cdot THICK + 1368.70 \end{aligned} \quad (2)$$

Table 2: Average relative deviations from experimental data for individual steel grades

Steel grade	Average relative deviation from experimental data [%]	Number of V-notch test pieces
20NiCrMo2	260.95 %	6
33MnCrB5-2	186.73 %	2
16MnCrS5	147.46 %	16
C45	134.50 %	25
33MnCrNiMoB5	116.28 %	4
16MnCr5	92.13 %	1
28MnCrNiB	70.00 %	13
C35S	55.36 %	25
C45S	44.44 %	15
C22	40.35 %	5
38MnVS6	39.78 %	143
42CrMoS4	37.82 %	56
28MnCrB7	36.45 %	78
S355J2	35.75 %	572
46MnVS5	35.63 %	13
25CrMo4	33.15 %	4
P460NH	31.42 %	197
25CrMoS4	26.28 %	30
23MnNiCrMo5-2	24.01 %	36
S235J2	23.88 %	22
42CrMo4	22.23 %	14
S235JR	20.80 %	8
41CrS4	17.82 %	2
20MnV6	13.82 %	934
30MnB5	13.23 %	19
41Cr4	9.37 %	1
18CrNiMo7-6	8.76 %	2
Total	29.05 %	2243

The average relative deviation from the experimental data is 29.05 %. The average relative deviations from the experimental data for individual steel grades are pre-

sented in **Table 2**. Based on the analyzed deviations between the predicted and experimental data, the largest difference occurred for 20NiCrMo2 steel grade, where only 6 V-notch pieces were used for Charpy pendulum impact testing. This deviation can be attributed to the degree of segregation due to the higher concentration of alloying elements.

Table 3 shows the average relative deviations from the experimental data for the rolled material diameter/thickness. The decrease in the prediction accuracy is clearly visible for larger dimensions. This deviation can be attributed to the development and the size of dendritic and equiaxed zone.

Table 3: Average relative deviation from experimental data for rolled material diameter/thickness

Thickness/diameter [mm]	Average relative deviation from experimental data [%]	Number of V-notch test pieces
10	22.42 %	1287
20	34.58 %	378
30	38.46 %	139
40	40.21 %	176
50	25.85 %	79
60	30.15 %	22
70	48.84 %	76
80	46.54 %	31
90	53.57 %	55
Total	29.05 %	2243

Table 4 shows the average relative deviation from the experimental data for the test temperature. The decrease in the prediction accuracy is clearly visible for lower temperatures. Deviations in highly alloyed steels (i.e., higher alloying contents) and deviations attributed to steel solidification (i.e., continuous casting) are even more pronounced at lower temperatures.

Table 4: Average relative deviation from experimental data for test temperature (TEMP)

Test temperature [°C]	Average relative deviation from experimental data [%]	Number of V-notch test pieces
–60.0	108.08 %	11
–50.0	89.84 %	25
–40.0	42.13 %	272
–30.0	11.06 %	825
–20.0	36.44 %	595
20.0	38.39 %	515
Total	29.05 %	2243

Unfortunately, based on the above data, it is not easy to conclude how the total alloying element content or the number of samples affect the prediction of absorbed energy using linear regression.

However, the following diagram (**Figure 5**) shows the effects of individual parameters calculated using the obtained linear regression model on the absorbed energy of V-notch test pieces. The casting parameters include the average cooling water flow in the first (QZ1) and the second zone (QZ2) of secondary cooling, which affect the development of dendritic and equiaxed zone (macro-structures) in the cast billets. The chemical elements include carbon (C), molybdenum (Mo) and nickel (Ni). The same diagram also shows that the test temperature (TEMP) drastically affects the impact test results.

Based on the calculations of the effects of individual parameters and the shown average relative deviation from the experimental data, we can conclude that the macrostructure of the billets and the associated sampling locations (i.e., locations of test pieces) drastically affect the impact test results.

3.2 Modeling of absorbed energy using genetic programming

In genetic programming, which is one of the most general evolutionary optimization methods,[31,32] the organisms that undergo adaptation are in fact mathematical expressions (models). These models consist of selected functions (e.g., basic arithmetical functions) and terminal genes (e.g., independent input parameters, and random floating-point constants). Typical function genes are: addition (+), subtraction (-), multiplication (*), division (/), and terminal genes (e.g., x, y, z). Random computer programs for calculating various forms and lengths are generated by means of selected genes at the beginning of the simulated evolution. The varying of the computer programs is carried out by means of genetic operations (e.g., crossover, mutation) during several iterations, called generations. After the completion of the variation of the computer programs, a new generation is obtained. Each result obtained from an individual program in a generation is evaluated against the experimental data. The process of changing and evaluating organisms is repeated until the termination criterion of the process is fulfilled.

The in-house built genetic programming system, programmed using AutoLISP, integrated into AutoCAD (i.e., commercial computer-aided design software), was used.[33–35] Its settings were as follows:

- the size of the population of organisms: 1000;
- the maximum number of generations: 100;

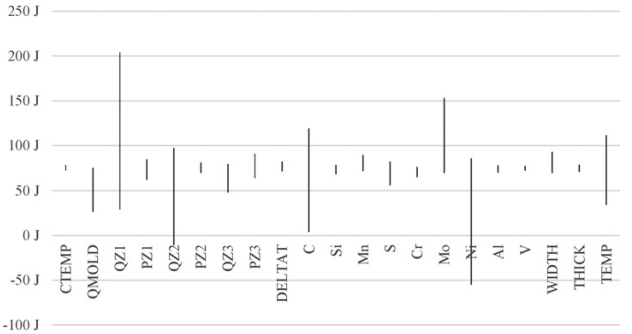

Figure 5: Effects of individual parameters calculated using the obtained linear regression model

- reproduction probability: 0.4;
- crossover probability: 0.6;
- the maximum permissible depth in the creation of the population: 30;
- the maximum permissible depth after the operation of crossover of two organisms: 30; and
- the smallest permissible depth of organisms in generating new organisms: 2.

Genetic operations of reproduction and crossover were used. For the selection of organisms, the tournament method with tournament size 7 was used.

The best developed model is:

KV = 1361.05 – 72.052·Al-2-9.899·C-0.095·CTEMP – 1.997·DELTAT – 13.539·Mn+1+ 7.017·Mo-9-0.117·Ni-6-806·PZ1 + 1.1·PZ3 – 0.573·QMOLD – 8.477·QZ1 + + .122·QZ2 + 0.547·QZ3 + 0.965·TEMP + 3.395·AlTHICK – 35.627·Mn·V0.143·Mn·WIDTH + WIDTH (96.974 + 0.143·Al + 157.017·Mo + DELTAT·TEMP + Al·Cr·PZ3·QZ3 (–7.561·TEMP – 0.082·THICK)) / (– QMOLD + WIDTH) – WIDTH (0.082·THICK – 0.082·Al·THICK + 261.564·Al·THICK – 35.627·V – 35.627·Al·PZ3·V + 2.143·WIDTH)/ (–QMOLD + WIDTH) (3)

with an average relative deviation from the experimental data of 25.52 %. Based on the analyzed deviations between the predicted and experimental data, the largest difference occurred for the 20NiCrMo2 steel grade in the linear regression model, where the average relative deviation was 260.95 %, compared to 203.48 % for the genetic programming model.

Table 5: Average relative deviation from experimental data for individual steel grades

Steel grade	Average relative deviation from experimental data [%]	Number of V-notch test pieces
20NiCrMo2	203.48 %	6
33MnCrB5-2	173.31 %	2
16MnCrS5	136.71 %	16
33MnCrNiMoB5	118.63 %	4
28MnCrNiB	99.92 %	13
16MnCr5	82.56 %	1
C45S	59.60 %	15
C45	48.36 %	25
41Cr4	35.52 %	1
C35S	34.70 %	25
28MnCrB7	33.42 %	78
42CrMoS4	32.28 %	56
P460NH	31.34 %	197
S355J2	30.52 %	572
25CrMo4	29.79 %	4
S235J2	29.61 %	22
Overall	29.05 %	2243
41CrS4	28.94 %	2
S235JR	27.80 %	8
38MnVS6	27.70 %	143
25CrMoS4	26.50 %	30
30MnB5	25.17 %	19
42CrMo4	24.84 %	14
23MnNiCrMo5-2	23.74 %	36
C22	20.20 %	5
46MnVS5	20.03 %	13
20MnV6	13.60 %	934
18CrNiMo7-6	10.62 %	2
Total	25.52 %	2243

Table 3 shows the average relative deviation from the experimental data for the rolled material diameter/thickness. As in the linear regression model, the decrease in the prediction accuracy is also visible for larger dimensions. In the linear regression model, the average relative deviation for the largest dimension of 90 mm was 53.57 %, while in the genetic programming model, it was 40.53 %.

Table 6: Average relative deviation from experimental data for rolled material diameter/thickness

Thickness/diameter [mm]	Average relative deviation from experimental data [%]	Number of V-notch test pieces
10	19.33 %	1287
20	31.37 %	378
30	35.24 %	139
40	38.61 %	176
50	22.10 %	79
60	27.38 %	22
70	39.97 %	76
80	38.52 %	31
90	40.53 %	55
Total	25.52 %	2243

Table 4 shows the average relative deviation from the experimental data for the test temperature. The decrease in the prediction accuracy is clearly visible at lower temperatures. In the linear regression model, the average relative deviation for the lowest test temperature of –60.05 °C was 108.08 %, while in the genetic programming model it was 78.57 %.

Table 7: Average relative deviation from experimental data for test temperature (TEMP)

Test temperature [°C]	Average relative deviation from experimental data [%]	Number of V-notch test pieces
–60.0	78.57 %	11
–50.0	63.54 %	25
–40.0	37.26 %	272
–30.0	11.05 %	825
–20.0	33.12 %	595
20.0	30.11 %	515
Overall	25.52 %	2243

Similarly to what we showed with the linear regression model, the following diagram (**Figure 6**) illustrates

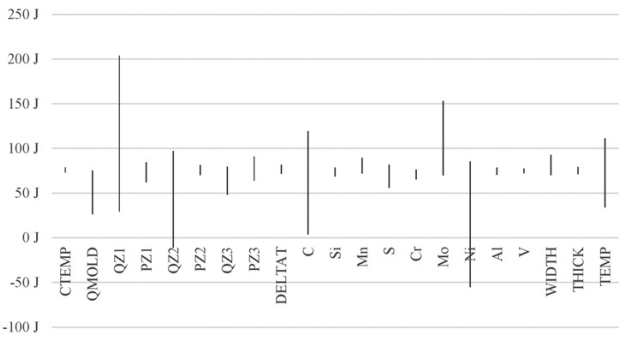

Figure 6: Effects of individual parameters calculated using the obtained linear regression model

the effects of individual parameters, calculated using the obtained genetic programming model, on the absorbed energy of V-notch test pieces. The average cooling water flow in the first (QZ1) and the second zone (QZ2) of secondary cooling and the contents of carbon (C), molybdenum (Mo) and nickel (Ni) are most influential. At the same time, the test temperature (TEMP) shows similar effects.

Based on the calculations of the effects of individual parameters using the linear regression and genetic programming models and the above average relative deviation from the experimental data, it is clear that the macrostructure of the billets and the associated sampling location (i.e., location of test pieces) drastically affect the impact test results. Consequently, consistency in the preparation of test pieces from the sample (i.e., a rough specimen) is essential.

5 CONCLUSIONS

This article presents the prediction of absorbed energy, based on 2243 V-notch test pieces obtained from rolled material produced (without additional heat treatment) in batches of several hypoeutectoid steels at Štore Steel Ltd. between January 2019 and May 2024, using linear regression and genetic programming.

The data on chemical composition (contents of C, Si, Mn, S, Cr, Mo, Ni, Al, and V), width and thickness of the rolled bar and test temperature (from –60 °C to 20 °C) were gathered for the prediction of absorbed energy. Special emphasis was placed on the casting parameters (i.e., average casting temperature, mold water flow, average difference between input and output mold cooling water temperature, average cooling water flow and pressure in three zones of secondary cooling) and the associated macrostructure of the cast semi-product.

On the basis of the collected data, the prediction of absorbed energy for V-notch test pieces was conducted using linear regression and genetic programming. For the fitness function, the average relative deviation between the predicted and experimental data was selected.

The average relative deviation from the experimental data was 29.05 % in the linear regression model and 25.52 % in the genetic programming model. Based on the analyzed deviations between the predicted and experimental data, the largest difference occurred for the 20NiCrMo2 steel grade in the linear regression model, where the average relative deviation was 260.95 %, while in the genetic programming model, it was 203.48 %. This deviation can be attributed to the degree of segregation due to the higher alloying content. A decrease in the prediction accuracy was observed for larger dimensions. The deviation can also be attributed to the development and size of the dendritic and equiaxed zone. In the linear regression model, the average relative deviation for the largest dimension of 90 mm was 53.57 %, while in the genetic programming model, it was 40.53 %. Similarly, in the linear regression model, the average relative deviation for the lowest test temperature of –60.05 °C was 108.08 %, while in the genetic programming model, it was 78.57 %. Deviations in highly alloyed steels (i.e., higher alloying contents) and deviations attributed to steel solidification (i.e., continuous casting) were even more pronounced at lower temperatures.

Based on the calculations of the effects of individual parameters on the absorbed energy of V-notch test pieces using the linear regression and genetic programming model, we can conclude that the casting parameters (average cooling water flow in the first and the second zone of secondary cooling), which affect the development of the dendritic and equiaxed zone (macro-structures) in the cast billets, the chemical composition (carbon, molybdenum and nickel contents) and the test temperature are most influential factors. Consequently, the location, orientation, and preparation of the test pieces are essential.

For future analysis, we will include the macroetching of rolled bars used for V-notched test specimens, focusing primarily on the specimens' location and uniform preparation.

Acknowledgment

This research was funded by the Slovenian Research and Innovation Agency, grant number L2-3173.

6 REFERENCES

[1] ISO 148-1 – Metallic materials – Charpy pendulum impact test, 2016, 29, Available at: https://www.iso.org/standard/63802.html

[2] M. Kovačič, B. Šarler, Batch-filling scheduling and particle swarms, Mater. Tehnol., 46 (2012) 3

[3] R. Muscat, M. Mahfouf, Predicting Charpy Impact Energy for Heat-Treated Steel Using a Quantum-Membership-Function-Based Fuzzy Model, IFAC-PapersOnLine, 49 (2016), 138–142, Available at: https://linkinghub.elsevier.com/retrieve/pii/S2405896316316731

[4] M. Kunigita, S. Aihara, T. Kawabata, T. Kasuya, Y. Okazaki, M. Inomoto, Prediction of Charpy impact toughness of steel weld heat-affected zones by combined micromechanics and stochastic fracture model – Part I: Model presentation, Eng. Fract. Mech., 230 (2020), 106965, Available at: https://linkinghub.elsevier.com/retrieve/pii/S001379441930801X

[5] J. Ren, Q. Chen, J. Chen, Z. Liu, Role of vanadium additions on tensile and cryogenic-temperature Charpy impact properties in hot-rolled high-Mn austenitic steels, Mater. Sci. Eng. A, 811 (2021), 141063, Available at: https://linkinghub.elsevier.com/retrieve/pii/S0921509321003324

[6] S. Hong, J. Lee, K. S. Park, s. Lee, Effects of boron addition on tensile and Charpy impact properties in high-phosphorous steels, Mater. Sci. Eng. A, 589 (2014), 165–173, Available at: https://linkinghub.elsevier.com/retrieve/pii/S0921509313010897

[7] H. K. Sung, S. Y. Shin, B. Hwang, C. G. Lee, N. J. Kim, S. Lee, Effects of carbon equivalent and cooling rate on tensile and Charpy impact properties of high-strength bainitic steels, Mater. Sci. Eng. A, 530 (2011), 530–538, Available at: https://linkinghub.elsevier.com/retrieve/pii/S0921509311011178

[8] Z. Száraz, P. Hähner, J. Stráská, S. Ripplinger, Effect of phase separation on tensile and Charpy impact properties of MA956 ODS steel, Mater. Sci. Eng. A, 700 (2017), 425–437, Available at: https://linkinghub.elsevier.com/retrieve/pii/S0921509317307736

[9] A. Ghosh, P. Modak, R. Dutta, D. Chakrabarti, Effect of MnS inclusion and crystallographic texture on anisotropy in Charpy impact toughness of low carbon ferritic steel, Mater. Sci. Eng. A, 654 (2016), 298–308, Available at: https://linkinghub.elsevier.com/retrieve/pii/S0921509315307437

[10] X. Zhou, C. Jia, P. Mi, et al., Cyclic quenching treatment doubles the Charpy V-notch impact energy of a 2.3 GPa maraging steel, J. Mater. Sci. Technol., 209 (2025), 311–328, Available at: https://linkinghub.elsevier.com/retrieve/pii/S1005030224005966

[11] J. Hure, A. Parrot, S. Meunier, Numerical prediction of the effect of irradiation on the Charpy Upper Shelf Energy of Reactor Pressure Vessel steels, J. Nucl. Mater., 570 (2022), 153956, Available at: https://linkinghub.elsevier.com/retrieve/pii/S0022311522004421

[12] S. Zhang, Y. Wang, M. Zhu, Z. Zhang, P. Nie, Z. Li, Relationships among Charpy impact toughness, microstructure and fracture behavior in 10CrNi3MoV steel weld joint, Mater. Lett., 281 (2020), 128328, Available at: https://linkinghub.elsevier.com/retrieve/pii/S0167577X20310338

[13] H. Kim, J. Park, M. Kang, S. Lee, Interpretation of Charpy impact energy characteristics by microstructural evolution of dynamically compressed specimens in three tempered martensitic steels, Mater. Sci. Eng. A, 649 (2016), 57–67, Available at: https://linkinghub.elsevier.com/retrieve/pii/S0921509315304378

[14] H. K. Sung, S. Y. Shin, B. Hwang, C. G. Lee, N. J. Kim, S. Lee, Effects of carbon equivalent and cooling rate on tensile and Charpy impact properties of high-strength bainitic steels, Mater. Sci. Eng. A, 530 (2011), 530–538, Available at: http://linkinghub.elsevier.com/retrieve/pii/S0921509311011178

[15] R. Meshkabadi, V. Pouyafar, R. Soltanikia, Investigation on Microstructure, Hardness and Fracture Energy of AISI H13 Hot Work Tool Steel by Cyclic Heat Treatment, J. Mater. Eng. Perform., 33 (2024), 6620–6629, Available at: https://link.springer.com/10.1007/s11665-023-08439-7

[16] X. Wang, O. Sanchez-Mata, S. E. Atabay, J. A. Muñiz-Lerma, M. Attarian Shandiz, M. Brochu, Crystallographic orientation dependence of Charpy impact behaviours in stainless steel 316L fabricated by laser powder bed fusion, Addit. Manuf., 46 (2021), 102104, Available at: https://linkinghub.elsevier.com/retrieve/pii/S2214860421002694

[17] Y. Cao, Y. Zhen, M. Song, H. Yi, F. Li, X. Li, Determination of Johnson–Cook parameters and evaluation of Charpy impact test performance for X80 pipeline steel, Int. J. Mech. Sci., 179 (2020), 105627, Available at: https://linkinghub.elsevier.com/retrieve/pii/S0020740319328644

[18] J. Mao, Q. Xu, J. Yang, et al., Nonlinear Impact Damage Evolution of Charpy Type and Analysis of Its Key Influencing Factors, Chinese J. Mech. Eng., 37 (2024) 3, Available at: https://cjme.springeropen.com/articles/10.1186/s10033-023-00986-3

[19] W. Jia, A. Pi, Z. Zhao, et al., Study on Intrinsic Influence Law of Specimen Size and Loading Speed on Charpy Impact Test, Materials (Basel), 15 (2022), 3855, Available at: https://www.mdpi.com/1996-1944/15/11/3855

[20] A. Hosseinzadeh, S. H. Hashemi, H. Rastegari, M. R. Maraki, Investigation of the notch depth effect on Charpy fracture energy and fracture surface features of API X65 steel, Can. Metall. Q., 62 (2023), 36–48, Available at: https://www.tandfonline.com/doi/full/10.1080/00084433.2022.2066241

[21] ISO 148-2 – Metallic materials – Charpy pendulum impact test, Part 2: Verification of testing machines, Available at: https://www.iso.org/standard/63812.html

[22] Y. Y. Yang, M. Mahfouf, G. Panoutsos, Probabilistic characterisation of model error using Gaussian mixture model–With application to Charpy impact energy prediction for alloy steel, Control Eng. Pract., 20 (2012), 82–92, Available at: https://linkinghub.elsevier.com/retrieve/pii/S0967066111001973

[23] M. Kovačič, U. Župerl, Modeling of Tensile Test Results for Low Alloy Steels by Linear Regression and Genetic Programming Taking into Account the Non-Metallic Inclusions, Metals (Basel), 12 (2022), 1343, Available at: https://www.mdpi.com/2075-4701/12/8/1343

[24] M. Park, G.-W. Park, S. Kim, et al., Tensile and Charpy impact properties of heat-treated high manganese steel at cryogenic temperatures, J. Nucl. Mater., 570 (2022), 153982, Available at: https://linkinghub.elsevier.com/retrieve/pii/S0022311522004688

[25] M. Cauwels, R. Depraetere, W. De Waele, S. Hertelé, K. Verbeken, T. Depover, Effect of hydrogen charging on Charpy impact toughness of an X70 pipeline steel, Procedia Struct. Integr., 42 (2022), 977–984, Available at: https://linkinghub.elsevier.com/retrieve/pii/S2452321622006801

[26] A. Biancalana Neto, H. J. C. Voorwald, Â. Caporalli Filho, M. F. Fernandes, E. S. Callisaya, A. Marinaro, Double vibratory stress relief treatment of welded pipes as an alternative to heat stress relief treatment: Effects on hardness, Charpy impact energy and CTOD, Int. J. Press. Vessel. Pip., 206 (2023), 105043, Available at: https://linkinghub.elsevier.com/retrieve/pii/S0308016123001606

[27] Y. Dubey, P. Sharma, M. P. Singh, Optimization using genetic algorithm of GMAW parameters for Charpy impact test of 080M40 steel, Int. J. Interact. Des. Manuf., 18 (2024), 6673–6683, Available at: https://link.springer.com/10.1007/s12008-023-01371-z

[28] R. Colas-Marquez, M. Mahfouf, Data Mining and Modelling of Charpy Impact Energy for Alloy Steels Using Fuzzy Rough Sets, IFAC-PapersOnLine, 50 (2017), 14970–14975, Available at: https://linkinghub.elsevier.com/retrieve/pii/S240589631733481X

[29] M. Mahfouf, Y. Y. Yang, A GA-Optimised Ensemble Neural Network Model For Charpy Impact Energy Predictions, IFAC Proc., 43 (2010), 62–67, Available at: https://linkinghub.elsevier.com/retrieve/pii/S1474667016328154

[30] S. Rath, S. K. Gond, P. Kumar, P. Sahana, S. K. Thakur, P. Pathak, Prediction of Impact Energy of Steel Using Artificial Neural Network, (2022), 274–283, Available at: https://link.springer.com/10.1007/978-3-031-22485-0_25

[31] J. R. Koza, Genetic Programming: On the Programming of Computers by Means of Natural Selection, Cambridge, MA, USA, MIT Press, 1992

[32] R. K. John, H. B. I. Forrest, A. David, A. K. Martin, Genetic Programming III: Darwinian Invention and Problem Solving, 1999

[33] M. Kovačič, U. Župerl, Genetic programming in the steelmaking industry, Genet. Program. Evolvable Mach., 21 (2020), 99–128, Available at: http://link.springer.com/10.1007/s10710-020-09382-5

[34] M. Kovačič, B. Šarler, Genetic programming prediction of the natural gas consumption in a steel plant, Energy, 66 (2014), 273–284, Available at: http://linkinghub.elsevier.com/retrieve/pii/S0360544214001340

[35] M. Kovačič, F. Dolenc, Prediction of the natural gas consumption in chemical processing facilities with genetic programming, Genet. Program. Evolvable Mach., (2016), Available at: http://link.springer.com/10.1007/s10710-016-9264-x